Conditional targeting of plectin in prenatal and adult mouse stratified epithelia causes keratinocyte fragility and lesional epidermal barrier defects

Reinhard Ackerl[1,*], Gernot Walko[1,*], Peter Fuchs[1], Irmgard Fischer[1], Matthias Schmuth[2] and Gerhard Wiche[1,‡]

[1]Department of Molecular Cell Biology, Max F. Perutz Laboratories, University of Vienna, 1030 Vienna, Austria
[2]Department of Dermatology and Venereology, Medical University of Innsbruck, 6020 Innsbruck, Austria

*These authors contributed equally to this work
‡Author for correspondence (e-mail: gerhard.wiche@univie.ac.at)

Accepted 15 May 2007
Journal of Cell Science 120, 2435-2443 Published by The Company of Biologists 2007
doi:10.1242/jcs.004481

Summary

Plectin, a widespread intermediate filament-based cytolinker protein capable of interacting with a variety of cytoskeletal structures and plasma membrane-bound junctional complexes, serves essential functions in maintenance of cell and tissue cytoarchitecture. We have generated a mouse line bearing floxed plectin alleles and conditionally deleted plectin in stratified epithelia. This strategy enabled us to study the consequences of plectin deficiency in this particular type of tissues in the context of the whole organism without plectin loss affecting other tissues. Conditional knockout mice died early after birth, showing signs of starvation and growth retardation. Blistering was observed on their extremities and on the oral epithelium after initial nursing, impairing food uptake. Knockout epidermis was very fragile and showed focal epidermal barrier defects caused by the presence of small skin lesions. Stratification, proliferation and differentiation of knockout skin seemed unaffected by epidermis-restricted plectin deficiency. In an additionally generated mouse model, tamoxifen-induced Cre-ER^{T}-mediated recombination led to mice with a mosaic plectin deletion pattern in adult epidermis, combined with microblister formation and epidermal barrier defects. Our study explains the early lethality of plectin-deficient mice and provides a model to ablate plectin in adult animals which could be used for developing gene or pharmacological therapies.

Supplementary material available online at
http://jcs.biologists.org/cgi/content/full/120/14/2435/DC1

Key words: Conditional gene targeting, Epidermolysis bullosa, Hemidesmosomes, Keratinocytes, Plectin, Transepidermal water loss

Introduction

Plectin, a highly versatile cytolinker protein, is essential in maintaining the integrity of skin, muscle and heart cytoarchitecture. It is expressed in a wide variety of mammalian cells and tissues and plays an important role in mediating interactions between different cytoskeletal network systems and their anchorage at cell-cell and cell-matrix junctional complexes (Wiche, 1998). In skin, as well as in cultured keratinocytes, plectin is predominantly localized at hemidesmosomes (HDs) and cell-cell borders (Andrä et al., 2003). Association of plectin with desmosomes (Eger et al., 1997) has been shown in simple epithelial cells. With an N-terminal actin-binding domain (Andrä et al., 1998), which serves also as an integrin β4 (Intβ4)-binding site (Rezniczek et al., 1998), and a C-terminal intermediate filament (IF)-binding site, plectin is instrumental in the physical anchorage of keratin filaments at the hemidesmosomal complex (Rezniczek et al., 1998; Andrä et al., 1997).

In humans, mutations in the plectin gene (*PLEC1*) result in skin fragility, manifested as blister formation at the level of HDs (for a review, see Pfendner et al., 2005). Clinically, these blistering disorders belong to the spectrum of epidermolysis bullosa (EB) phenotypes. Most plectin mutations lead to EB-MD, a condition characterized by neonatal blistering and late onset muscular dystrophy. Recently, however, plectin mutations have also been found in EB patients with pyloric atresia (EB-PA) (Pfendner and Uitto, 2005), a combination that can lead to early postnatal demise of the affected individuals.

Plectin-deficient mice die 1-3 days after birth exhibiting skin blistering caused by disruption of basal keratinocytes, as well as myopathies in skeletal muscle and disintegration of intercalated disks in the heart (Andrä et al., 1997). Rupture of basal keratinocytes occurs in the cytoplasm just above the inner hemidesmosomal plaque structures (Andrä et al., 1997).

The early lethality of plectin-null mice precluded the analysis of possible plectin functions at later stages of postnatal development and maturation of mice. To circumvent this problem we have now generated mice with floxed plectin alleles, rendering the plectin locus susceptible to conditional elimination by Cre recombinase. We describe here the skin phenotype of a mouse line showing a complete knockout of plectin restricted to keratin 5 (KRT5; hereafter referred to as K5)-expressing epithelia. In addition, we have generated an inducible mouse model, where plectin expression can be

knocked out in small patches of epidermis at the adult stage of the animal. Our analysis of these mice demonstrates the importance of plectin in mediating mechanical stress resistance of newborn and adult epidermis and offers an explanation for the early death of plectin-deficient animals.

Results

Generation of mice bearing floxed plectin alleles

We have previously shown that the inactivation of the plectin gene in the mouse germline results in postnatal death, with pups showing severe skin blistering as well as muscular dystrophy (Andrä et al., 1997). To assess whether the blistering of the epidermis, or of other stratified epithelia, was causing the animals' death, we used a gene-targeting approach to create mice with a constitutive knockout of plectin in stratified epithelia, but not in other types of tissues. Our targeting vector contained single *loxP* sites in introns 25 and 31, so that upon conditional removal of exons 26-31, exon 25 would be spliced into exon 32, leading to a frameshift and a premature stop codon (see Fig. S1A in supplementary material). Selected ES cell clones were screened for correct recombination events by Southern blotting (Fig. S1B in supplementary material) and subsequently injected into blastocysts. After germline transmission of the targeted allele (Fig. S1C, lane 1 in supplementary material), the resulting mouse line carrying one $Plec^{flox(neo)}$ allele and one $Plec^{+}$ allele was bred to Flp deleter mice to excise the FRT-flanked selection marker. Pups carrying the $Plec^{flox}$ allele were identified and then bred to homozygosity (Fig. S1C, lane 2 in supplementary material). Mice homozygous for the floxed plectin allele ($Plec^{flox/flox}$) appeared to be normal indicating that the genetic manipulation had not altered the function of plectin (data not shown).

Inactivation of the plectin gene in mouse skin leads to early postnatal death, caused by severe blistering of the oral epithelium

To inactivate plectin in the skin, we crossed $Plec^{flox/flox}$ mice with transgenic mice expressing the Cre-recombinase under the control of the K5 promoter (Tarutani et al., 1997). $Plec^{\Delta/\Delta}$:K5-Cre ($Plec^{\Delta/\Delta}$:Krt5-Cre) mice thus generated will be referred to as K5-Cre KO. They were born at the expected Mendelian ratios and died 1-3 days after birth. They showed severe skin detachment, especially on the fore- and hindlimbs (Fig. 1A,B), and in some cases around the mouth and nasal cavities; rarely, aplasia cutis of the forelimbs was also noted (not shown). The extent of phenotypic alterations exhibited before death varied among knockout mice. Most common was skin detachment at forepaws (Fig. 1A), but also large blisters reaching the size of up to 1 cm^2 were found at the upper extremities and in the armpits (Fig. 1B,C). Sometimes blisters were torn open (Fig. 1B). A histological examination revealed blister formation between the dermis and the superficial epidermal layers (Fig. 1D). Furthermore, macroscopically non-visible microblisters were revealed (not shown). K5-Cre KO animals were smaller than control animals, obviously due to a reduced gain in body weight during their short life span (Fig. 1E). $Plec^{flox/flox}$ mice lacking the K5-Cre transgene, $Plec^{+/flox}$ and $Plec^{+/+}$:K5-Cre mice did not show any pathological skin phenotype. Thus, $Plec^{flox/flox}$ mice lacking the K5-Cre transgene were used as controls. By the type of skin disorder, reduced body weight and postnatal death, K5-Cre KO mice were indistinguishable from plectin-null ($Plec^{-/-}$) mice (Andrä et al., 1997). Conditional knockout mice that were nursed at least once after their birth regularly exhibited blisters in their oral cavities (Fig. 1F). A detailed analysis of serial sections covering the entire oral cavities of these mice revealed on average three to four blisters on their palates and rarely, blister formation on their tongues was observed. By contrast, no signs of epithelial detachment were detected in proximal esophagus of K5-Cre KO mice (Fig. 1G-J). Oral blistering most probably impaired the food intake of K5-Cre KO mice, so that death due to malnutrition ensued, as has been suspected in the case of plectin-null mice (Andrä et al., 1997). Newly born K5-Cre KO pups were able to suckle milk initially, as indicated by the milk patch shining through the skin of pups (data not shown) and a milk-filled gut (Fig. 1L), similar to control pups (Fig. 1K). However, after initial food intake, subsequent intake seemed to be impaired due to formed blisters, since the stomachs of still-living 2-day-old K5-Cre KO pups were always empty (Fig. 1L, inset). The presence of milk in the stomach and the intestine of K5-Cre KO pups (Fig. 1L) after food intake showed that, as in control pups (Fig. 1K), the transport of coagulated milk was not obstructed. Therefore, it could be ruled out that the mutant mice suffered from pyloric atresia, characterized by congenital obstruction of the gastric outlet.

To detect small localized breaches in skin barrier we performed dye penetration assays with 1-day-old littermates. In contrast to control mice (Fig. 1M), K5-Cre KO pups showed numerous dark spots, especially on their heads and forelegs (Fig. 1N), indicating localized loss of barrier function. Measurements of transepidermal water loss (TEWL), to detect increased fluid loss through lesions, revealed a ~3.5-fold increase in TEWL value compared to intact skin (data not shown). However, no differences in TEWL values were observed between intact skin of K5-Cre KO and control pups, demonstrating the absence of intrinsic barrier defects in K5-Cre KO mice. A histological examination of stained spots revealed microlesions at various stages of wound healing (Fig. 1O,P). Most lesions had a histological appearance similar to that shown in Fig. 1O, with a thick, acanthotic and weakly differentiated new epidermis having formed under a crust that was still covered with the old (dead) epidermis. In some lesions, a thin, multilayered sheet of keratinocytes could be seen under the crust, indicating ongoing re-epithelialization (Fig. 1P). To test whether such lesions could be induced by trauma we applied mild mechanical stress in the form of consecutive tape strippings with D-Squame disks (a procedure normally used to sequentially remove stratum corneum layers), to the back skin of newborn K5-Cre KO and control mice, followed by dye penetration assays. Indeed, we found small blue-stained spots in 10-times stripped K5-Cre KO (Fig. 1R), but not in control skin (Fig. 1Q). Histological examination of stripped K5-Cre KO skin areas showed that stripping had induced basal keratinocyte cytolysis (Fig. 1S). Moreover, a few tape strippings were often enough to induce the formation of a large blister (Fig. 1T). When stronger adhesive tape (Tesa 3M) was used, one stripping was sufficient to remove the entire epidermis of the stripped area (not shown). Together, these data demonstrated an extreme fragility of K5-Cre KO epidermis.

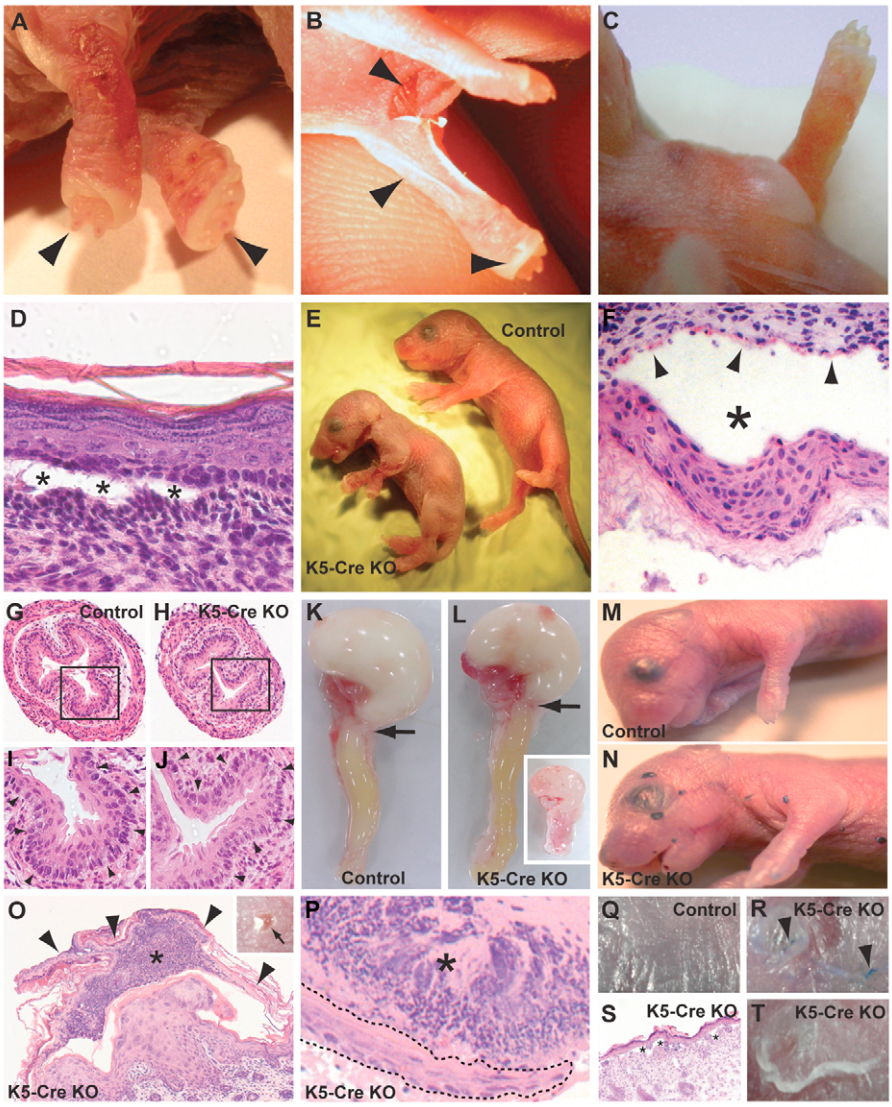

Fig. 1. Phenotypic analysis of K5-Cre KO mice. (A-C) Two-day-old K5-Cre KO pups showing severe skin detachments and skin lesions on their upper extremities and in their armpits. (D) Hematoxylin and Eosin (H/E) staining of K5-Cre KO skin, showing epidermal detachment (asterisks) at the level of the basal keratinocyte layer. (E) Size comparison of 2-day-old *Plec*$^{flox/flox}$ (control) and K5-Cre KO pups. (F) Huge blister (asterisk) detected in the upper palate of a 2-day-old K5-Cre KO pup. Parts of the epithelial tissue (arrowheads) are still attached to the connective tissue, indicating disruption of basal oral keratinocytes. (G-J) H/E stainings of cross sections of proximal esophagus from K5-Cre KO (H,J) and control mice (G,I). I and J show magnifications of the boxed areas in G and H, respectively. No detachment of the epithelium was observed. Arrowheads in I,J denote basement membrane. (K,L) Comparison of stomachs and upper intestines of newborn control and K5-Cre KO pups. Note the translocation of the milk from the stomach to the gut, showing that the K5-Cre KO pup has not been affected by pyloric atresia. The inset in L shows the empty stomach of a 2-day-old KO pup. Arrows point to the pyloric regions. (M,N) Toluidine Blue dye penetration assay. Note localized breaches in skin barrier of K5-Cre KO pups allowing penetration of dye. (O,P) Representative H/E stainings of Toluidine-Blue-stained spots, revealing microlesions. In O, note the newly formed acanthotic epidermis under a crust (asterisk) that is covered by pieces of the old (dead) epidermis (arrowheads). The inset in O shows a photograph of a microlesion (arrow). The lesion in P is in the process of re-epithelialization (dashed line). (Q-T) Induction of microlesions by mild trauma. Flank skins of newborn mice were tape-stripped 10 times and subsequently stained with Toluidine Blue (Q,R). Note blue-stained microlesions (arrowheads) in stripped skin of K5-Cre KO (R). Tape stripping caused epidermal detachment (S, asterisks) and blister formation (T) in K5-Cre KO skin.

Highly efficient reduction of plectin levels by K5-controlled Cre expression

To examine to what extent plectin expression was reduced in the epidermis of conditional knockout compared to control animals, immunoblotting of tissue homogenates was performed. Using an antiserum recognizing all isoforms of plectin (anti-pan-plectin), only a very weak, in fact barely detectable, signal was obtained in K5-Cre KO epidermis compared with the strong signal in control tissue (Fig. 2A). This remaining signal was likely to originate from non-keratinocyte cells present in the epidermis, such as dendritic (Langerhans) cells and pigment cells (melanocytes), which are known to express a set of plectin isoforms different from that of keratinocytes (Abrahamsberg et al., 2005) (our unpublished data). In fact, when an antiserum specific to plectin 1a, the major plectin isoform found in keratinocytes (Andrä et al., 2003), was used instead of the anti-pan-plectin antiserum, not even a weak signal was detectable in epidermal tissue extracts (data not shown). As expected, in tissue extracts from the dermis of K5-Cre KO animals, reduction of plectin expression was much less dramatic (Fig. 2A). Since neither the anti-plectin 1a nor the anti-pan-plectin antiserum (both recognizing epitopes in plectin domains preceding the rod), detected proteins in K5-Cre KO tissue homogenates, that were of lower molecular mass than full-length plectin, the expression of rodless-plectin in K5-Cre KO epidermis could be ruled out.

To examine the plectin gene locus of K5-Cre KO animals in Cre-affected (epidermal) tissue compared to putatively unaffected (dermal) tissue, DNAs isolated from epidermal and dermal K5-Cre KO tissues were subjected to Southern blot analysis, along with corresponding samples from control (*Plec*$^{flox/flox}$) animals. In K5-Cre KO epidermis, the only signal detected (9 kb) corresponded to the *Plec*$^{\Delta}$ allele, indicating a recombination efficiency of 100% (Fig. 2B). In K5-Cre KO dermis, however, the 15 kb wild-type signal was predominant, with an additional (lesser) signal of 9 kb (Fig. 2B). Considering that enzymatic detachment of the epidermis leaves some hair follicles embedded in the dermis (Vasioukhin et al., 1999) (our

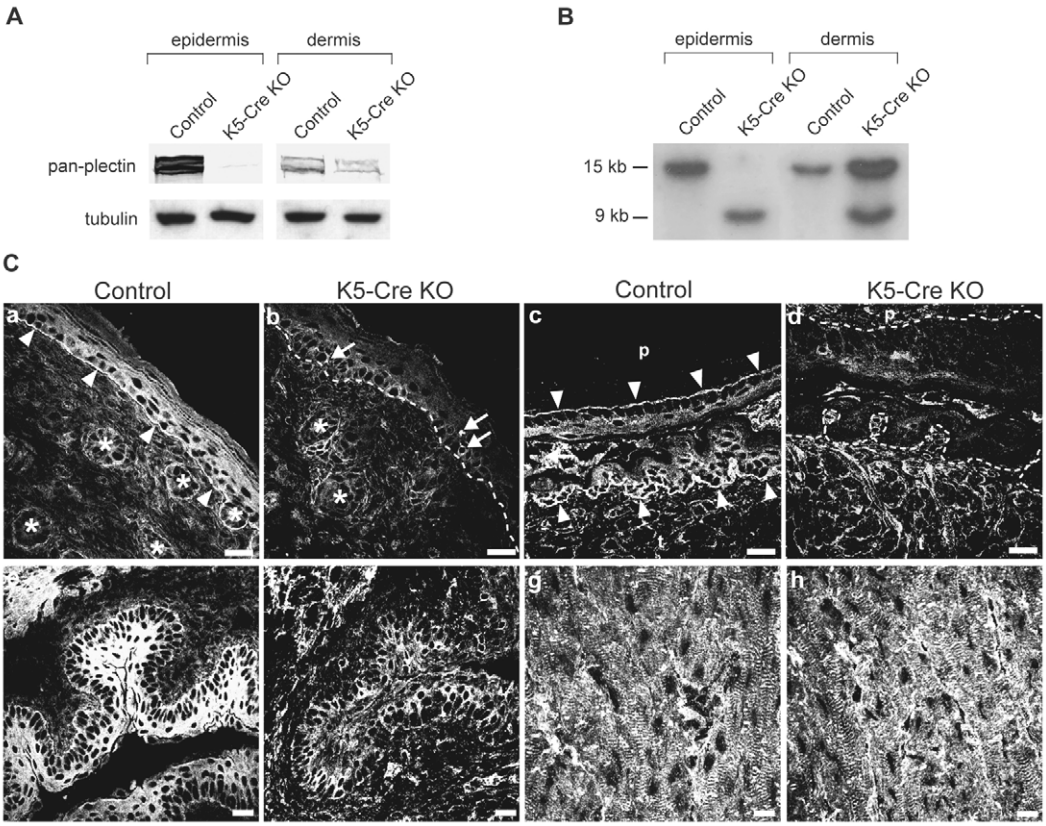

Fig. 2. High efficiency of Cre-mediated plectin deletion. (A) Immunoblotting of epidermal and dermal tissue homogenates from newborn *Plec*$^{flox/flox}$ (control) and K5-Cre KO mice. After separating epidermis and dermis using dispase, proteins were extracted and subjected to immunoblotting using anti-pan-plectin antiserum. Tubulin served as loading control. Note, very faint plectin signal in K5-Cre KO epidermis, testifying to nearly complete abolition of plectin in this tissue, whereas in dermis, plectin expression was hardly reduced. (B) Southern blot analysis of genomic DNAs from epidermis and dermis of newborn K5-Cre KO mice and their *Plec*$^{flox/flox}$ (control) littermates. DNAs were digested with *Nco*I (releasing 15 kb and 9 kb fragments from the *Plec*^{flox} and *Plec*$^{\Delta}$ alleles, respectively) and hybridized with the Nco probe (see Fig. S1A in supplementary material; *Plec*^{flox} and *Plec*$^{\Delta}$ alleles, respectively). Note complete conversion of the *Plec*^{flox} to the *Plec*$^{\Delta}$ allele in the epidermis of K5-Cre KO mice and the presence of some Cre activity in the dermis, as indicated by the 9 kb *Plec*$^{\Delta}$ allele. (C) Immunofluorescence microscopy of frozen skin (a,b), tongue and palate (c,d), esophagus (e,f) and heart (g,h) tissue sections of newborn control and K5-Cre KO specimens using anti-pan-plectin antiserum. Note strong plectin signal in control skin along the basal membrane (arrowheads in a) and throughout the epidermis. In the oral cavity, the plectin signal is most prominent along the basal membranes of palate and tongue epithelia (arrowheads in c). Plectin was also expressed in the dermis, foremost at dermo-epidermal junctions of hair follicles (asterisks in a). No plectin-specific label was detectable in K5-Cre KO epidermis, palate, and tongue epithelia, except for a few single epidermal cells, most likely melanocytes and Langerhans cells (arrows in b). Also note strongly reduced plectin-specific label in K5-Cre KO esophagus (f), but in K5-Cre KO heart, plectin expression was not reduced (h). p, palate; t, tongue. Dashed lines (in b and d) indicate dermo-epidermal borders. Bars, 20 μm.

unpublished observation), it is likely that the recombination signal observed in K5-Cre KO dermis stemmed from a contamination with keratinocytes. The absence of the 9 kb mutated gene signal in both controls (epidermis and dermis) indicated that aberrant (non-Cre-mediated) recombination between the *loxP* sites did not occur.

Additionally, we used immunofluorescence microscopy to assess the absence of plectin from the epidermis of knockout mice (Fig. 2C). A pronounced staining of the dermo-epidermal borderline, along with a weaker staining of the cytoplasm and membranes of all epidermal keratinocytes, was detected in normal mouse skin (Fig. 2Ca) but in the corresponding K5-Cre KO tissue, staining above background was observed in only a few insular cells (arrows in Fig. 2Cb). These plectin-positive cells most likely are melanocytes (especially those between and underneath basal keratinocytes and around hair follicles) and dendritic cells (in the suprabasal keratinocyte layers) which do not express K5 (Mahrle et al., 1989), and consequently no Cre recombinase. Plectin was also absent from the oral epithelia of K5-Cre KO animals (Fig. 2Cd), whereas in the oral cavity of wild-type mice it was strongly expressed along the basal membranes of palate and tongue epithelia (Fig. 2Cc), both of which express K5 at high levels. Plectin expression was also strongly reduced in esophagus (Fig. 2Cf), where K5 is expressed at high levels (Byrne and Fuchs, 1993), but not in the pseudostratified epithelium of the trachea (Fig. S2A,B in supplementary material), where K5 expression is restricted to a small subset of airway epithelial cells (Schoch et al., 2004) (also see Fig. S2C,D in supplementary material). As expected, plectin expression in heart (Fig. 2Ch) and skeletal muscle (data not shown) of K5-Cre KO mice was not affected.

Unaltered epidermal stratification and differentiation in K5-Cre KO mice

To investigate whether plectin deficiency had any influence on skin development and differentiation we undertook a detailed immunohistological analysis of skin sections from 1-day-old K5-Cre KO and control mice. First, we assessed the expression of two major hemidesmosomal proteins, Intβ4, which binds directly to plectin (Rezniczek et al., 1998), and BPAG1 (also known as dystonin; Dst). As expected, the Intβ4 signal was found confined to the basal membrane of basal keratinocytes and the outer root sheath of hair follicles (Fig. 3A,B). Similar

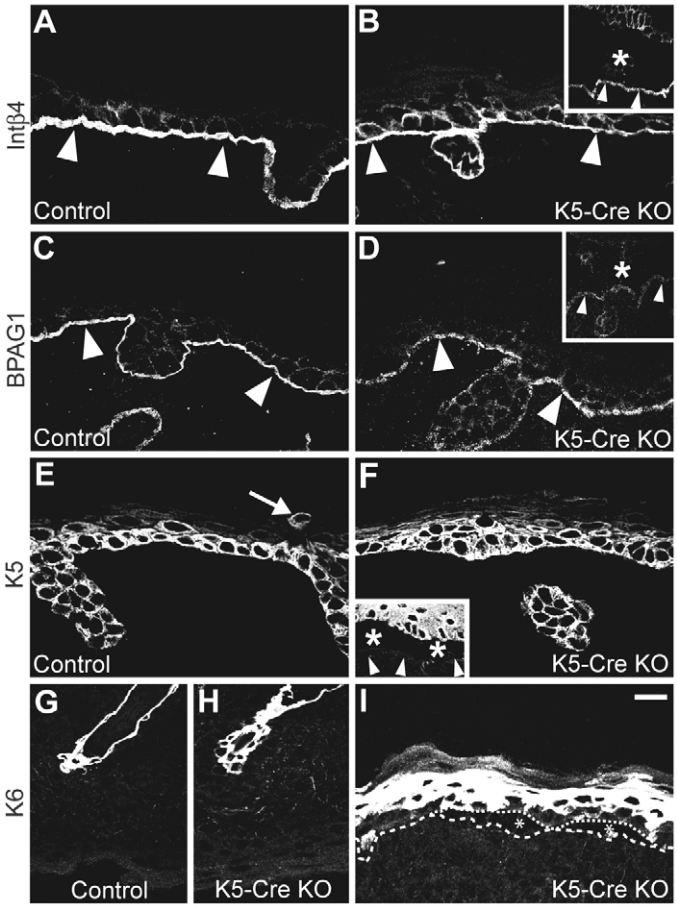

Fig. 3. Immunolocalization of Intβ4 (A,B), BPAG1 (C,D), K5 (E,F) and K6 (G-I) in skin sections from 1-day-old *Plec*$^{flox/flox}$ (control) and K5-Cre KO mice. (A,B) In control epidermis, the Intβ4 signal was confined to the basal membrane (arrowheads) of basal keratinocytes and the outer root sheath of hair follicles, whereas in K5-Cre KO epidermis, it was slightly reduced and less polarized. In blistered areas (inset in B, asterisk), Intβ4 was located at blister floors. (C,D) Note more discontinuous BPAG1 staining along basal keratinocyte membranes (arrowheads) in K5-Cre KO compared to control epidermis. Inset in D shows BPAG1 localization at the floor (arrowheads) of blisters (asterisk). (E,F) The K5 signal was restricted to basal keratinocytes and rare transit amplifying cells (arrow), without noticable differences between control and K5-Cre KO epidermis. In blistered areas (inset in F, asterisks), K5 was located at blister roofs (arrowheads denote the blister floor). (G-I) In control skin, K6 was exclusively expressed in hair follicles (G), while in leg skins of K5-Cre KO mice, in addition to hair follicles (H), patches of suprabasal keratinocytes above microblisters were K6-positive (I). In I the dashed line indicates the dermo-epidermal border and the dotted line, a microblister separating the epidermis from the underlying dermis. Asterisks, blister. Bar, 20 μm.

to plectin-null mice (Andrä et al., 1997), the Intβ4 signal was slightly weaker in the K5-Cre KO epidermis compared to controls (Fig. 3B). This observation was confirmed by immunoblotting data showing reduced Intβ4 levels in detergent resistant, keratin-containing cell fractions from trunk skin of K5-Cre KO mice (see Fig. S3B in supplementary material). In addition, in the absence of plectin the localization of Intβ4 seemed to be less polarized, since the protein was also found at lateral cell borders of basal keratinocytes (Fig. 3B). In blistered areas, the Intβ4 signal was located at blister floors, indicating disruption of basal keratinocytes at the level of the inner hemidesmosomal plaque (inset in Fig. 3B). BPAG1 staining at the basal surface membrane of K5-Cre KO keratinocytes was well preserved, although it appeared slightly more patchy than in the control samples (Fig. 3C,D). Similar to Intβ4, in blistered areas, the BPAG1 signal was located at the blister floor (inset in Fig. 3D). K5, the cytoskeletal binding partner of hemidesmosomal plectin, was faithfully located in the basal keratinocyte cell layer as well as in transit amplifying cells (arrow in Fig. 3E), with similar fluorescence intensities in control and K5-Cre KO specimens (Fig. 3E,F). In blisters, K5 was localized in blister roofs (inset in Fig. 3F). Regarding K6, which is normally expressed in hair follicle keratinocytes and in some basal and suprabasal keratinocytes in ridged skin (Swensson et al., 1998), we found expression in the companion layer of epidermal hair follicles without any difference between K5-Cre KO and control animals (Fig. 3G,H). However, consistent with its known upregulation under pathological and hyperproliferative conditions (Coulombe et al., 2004), K6 was found strongly upregulated in areas of K5-Cre KO fore- and hindleg tissue, where the epidermis had become detached from the dermis (Fig. 3I). Similar observations were previously reported for other mouse models of skin blistering diseases (Dowling et al., 1996; Peters et al., 2001; Raymond et al., 2005). In addition, our observation was confirmed by immunoblotting data revealing increased expression levels of K6 in knockout compared to wild-type skin (Fig. S3B).

Apart from HDs, actin-linked adherens junctions (AJs) and desmosomes have central functions in establishing the epithelial sheet and its polarity (Green and Gaudry, 2000). However, AJ formation appeared to be normal in K5-Cre KO epidermis as visualized using antibody (E-cadherin) and phalloidin (actin) labeling (see Fig. S4A-D in supplementary material), whereas desmoplakin staining revealed a slight reduction of desmosome structures in suprabasal epidermal cell layers of K5-Cre KO epidermis (Fig. S4E,F in supplementary material). Similar trends were observed by immunoblotting (Fig. S3B in supplementary material). However, when macroscopically intact K5-Cre KO backskin was subjected to electron microscopy, neither desmosomal structures nor anchored keratin filaments showed any abnormalities (data not shown).

Finally, we examined the differentiation capacity of knockout epidermis by tracing K10 and involucrin as early and late differentiation markers. However, no differences in the staining patterns of either K10 or involucrin were detectable in control and K5-Cre KO keratinocytes (see Fig. S5A-D in supplementary material), indicating that epidermal stratification and differentiation proceeded normally in the mutant mice.

Plectin-deficiency does not affect proliferation and survival of keratinocytes

To investigate whether plectin deficiency affects epidermal proliferation, sections of leg skin from 1-day-old wild-type and knockout mice were immunostained using antibodies to Ki-67 (see Fig. S6A,B in supplementary material). A statistical analysis carried out in nonlesional areas of interfollicular

epidermis showed that similar numbers of stained cells were present per linear millimeter of basal membrane, namely 58±13.1 and 61±14.3 for wild-type and knockout, respectively (Fig. S6C in supplementary material). This result indicated that plectin deficiency did not affect proliferation of keratinocytes in vivo. We also examined the effects of plectin deficiency on apoptosis by TUNEL analysis of the skin of newborn mice. Neither K5-Cre KO basal keratinocytes, nor control cells showed signs of apoptotic cell death (Fig. S6D,E in supplementary material). Occasionally, singular TUNEL-positive cells lining the exposed epidermal surface of blister roofs were found in K5-Cre KO mice (data not shown), indicating the occurrence of some apoptotic events after epidermal detachment.

Inducible knockout of plectin in adult skin leads to increased epidermal fragility and lesional barrier defects

Since K5-Cre KO mice, similar to plectin-null mice, died within a few days after birth, they were not suitable as an animal model for studying consequences of plectin loss at later stages in life. To overcome these limitations, we employed conditional gene targeting, using the Cre-*loxP* recombination system with an inducible chimeric Cre-ER^T recombinase that can be activated by 4-hydroxy-tamoxifen (OHT), but not by endogenous estradiol (Feil et al., 1996; Indra et al., 1999). To achieve temporally controlled somatic plectin ablation in the epidermis, we crossed mice with one floxed and one null allele (*Plec*$^{flox/–}$) with transgenic mice expressing the chimeric Cre-ER^T recombinase under the control of the bovine K5 promoter (Feil et al., 1996). Resulting mice with a *Plec*$^{flox/–}$:K5-Cre-ER^T genotype were injected intraperitoneally with 1 mg OHT per day for five consecutive days and were subjected to phenotypic analyses 2 weeks after the last injections. Southern blotting analysis showed that ~35% of the floxed plectin allele was converted to the Δ allele under these conditions (Fig. 4A).

Immunofluorescence microscopy of frozen tissue sections, using anti-pan-plectin antiserum, revealed that plectin deletion in skin was in fact mosaic. In leg as well as in tail and ear skin, large patches of epidermis expressing plectin were interspersed with small patches lacking plectin expression (Fig. 4B-D). Histological analysis of sections from tail and shaved back skin revealed normal organization of the epidermis and the absence

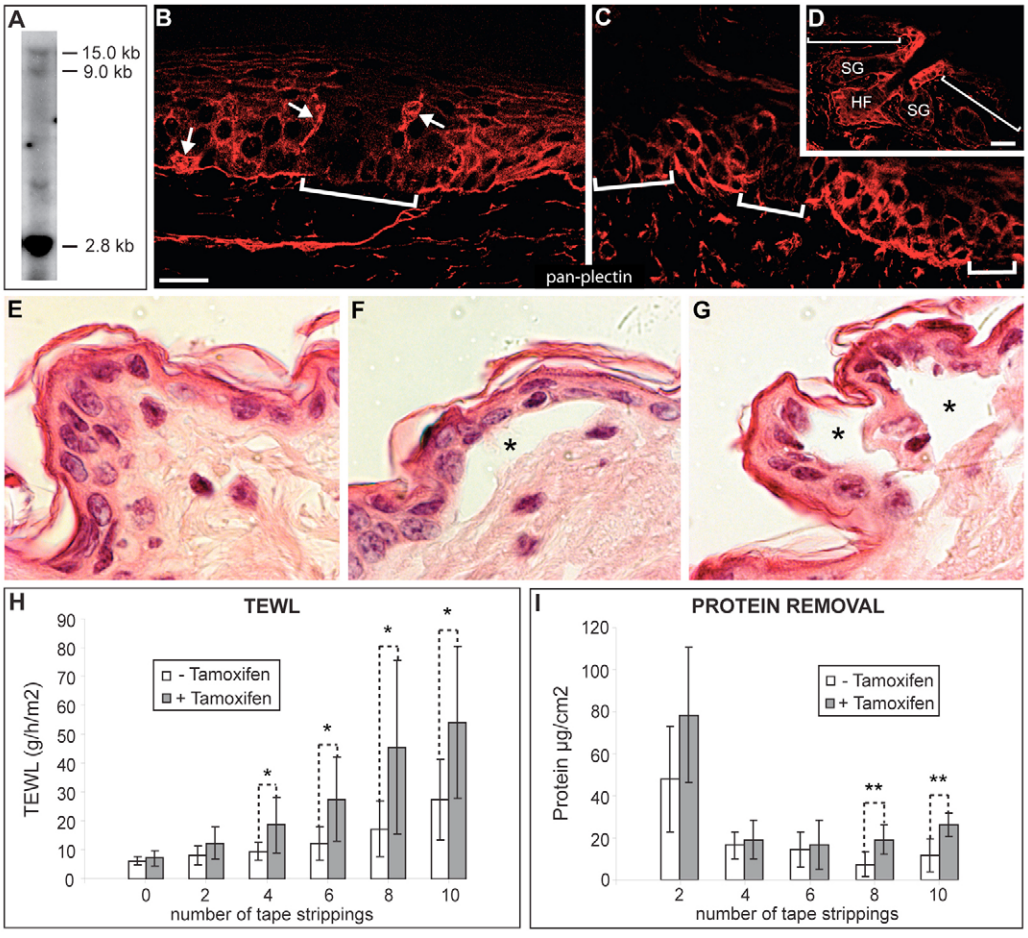

Fig. 4. Inducible knockout of plectin in mice and examination of epidermal integrity. (A) Southern blot analysis (autoradiography) of DNA isolated from the epidermis of a *PLEC*$^{flox/–}$:K5-Cre-ER^T mouse after treatment with 4-hydroxy-tamoxifen (OHT). DNA was digested with *Nco*I as described in Fig. 2, and hybridized with the Nco probe shown in Fig. S1A. The 2.8 kb signal stems from the plectin-null allele. Note partial Cre-mediated recombination after OHT treatment. (B-D) Immunofluorescence microscopy of frozen leg (B), ear (C) and tail (D) skin sections of OHT-treated *PLEC*$^{flox/–}$:K5-Cre-ER^T mouse specimens using anti-pan-plectin antiserum. Note patches of plectin-deficient keratinocytes in intrafollicular epidermis (brackets). Arrows in B indicate non-keratinocyte plectin-positive cells, most likely melanocytes and Langerhans cells. HF, hair follicle. SG, sebaceous gland. (E-G) H/E stainings of tail skin (E,F) and shaved back skin (G) specimens from OHT-treated *PLEC*$^{flox/–}$:K5-Cre-ER^T mice, showing normal skin morphology and absence of microblisters in unstressed skin (E) and formation of microblisters (asterisks) after repeated (10×) tape strippings with D-Squame disks (F,G). (H,I) Transepidermal water loss (TEWL; H) and quantification of stratum corneum protein removal (I) after serial tape strippings of skins from *Plec*$^{flox/–}$:K5-Cre-ER^T mice, that had been either untreated (–OHT) or treated (+OHT). Basal TEWL was measured before the first stripping. Values are mean ± s.e.m. from 5 OHT-treated and 5 untreated (control) *Plec*$^{flox/–}$:K5-Cre-ER^T littermates. Measurements were taken after two subsequent tape strippings. For statistical analyses the Student's *t*-test was used (**P*<0.1; ***P*<0.05). Note that for quantification of stratum corneum protein removal, disks from two subsequent strippings were pooled. Bars, 20 μm.

of microblisters (Fig. 4E). However, small blisters could be induced by repeated tape strippings using D-Squame disks (Fig. 4F,G), indicating that localized (mosaic) plectin deficiency made the epidermis of adult mice more susceptible to mechanical stress, although the plectin-expressing cells were sufficient to prevent epidermal detachment.

To quantify any focal defects in epidermal barrier function, we measured TEWL before and during acute barrier disruption by repeated tape strippings, as described above for constitutive conditional plectin knockout mice. In addition, the amount of proteins removed by serial tape strippings was measured to analyze stratum corneum cohesion. Under basal (non-stripped) conditions, animals with induced mosaic plectin deletion did not show a difference in TEWL, compared to control animals (Fig. 4H). However, after four subsequent strippings, TEWL began to increase sharply in mice with induced plectin deletion, but only modestly in control mice (Fig. 4H). No differences in TEWL could be observed between non-induced *Plec*$^{flox/-}$:K5-Cre-ER^{T}and non-induced *Plec*$^{flox/flox}$:K5-Cre-ER^{T} mice either under basal conditions or after tape stripping (data not shown). Estimates of the amount of proteins removed after each stripping demonstrated that during the last strippings proportionally more cells had been removed from the skin of mice with induced mosaic plectin deletion compared to control mice, suggesting increased fragility of the cell layers adjacent to the induced lesions (Fig. 4I). Overall, the data obtained with the inducible mouse model demonstrated that even localized plectin deficiency in the epidermis renders keratinocytes more prone to mechanical stress-inflicted damage.

Discussion

Similar to plectin-null mice, K5-Cre KO mice with a specific deletion of plectin in stratified epithelia died within 1-3 days postnatally exhibiting severe skin fragility, focal skin barrier defects and growth retardation. Focal skin barrier defects appeared to arise as a consequence of localized keratinocyte cytolysis and thus did not imply a direct role of plectin in barrier formation. Similar skin lesions with increased TEWL have previously been reported for desmocollin 1-null mice (Chidgey et al., 2001) where they were related to localized acantholysis. Small Toluidine-Blue-stained lesions were also found in the skin of K5 knockout mice, where they were attributed to cytolysis of basal keratinocytes (Peters et al., 2001). The early onset of blister formation and the severity of tissue fragility clearly showed that plectin is more important than BPAG1 in linking keratin filaments to hemidesmosomes, as BPAG1 knockout mice grow to adulthood and display only mild blistering (Guo et al., 1995). Apart from the formation of blisters and lesions due to epidermal detachment, the epidermis of K5-Cre KO displayed a normal stratified organization and correct expression patterns of differentiation markers, and proliferation and survival of keratinocytes were unaffected. The occasional presence of apoptotic cells in the lumen-proximal keratinocyte layer of blister roofs indicated that, although cytolysis due to keratinocyte disruption above the HDs predominated, some still intact keratinocytes underwent programmed cell death. However, massive apoptosis of basal keratinocytes, as it was observed upon epidermal detachment in Intβ4-deficient mice (Dowling et al., 1996; DiPersio et al., 2003), was not evident.

The skin phenotype of K5-Cre KO mice resembled that of children suffering from EB-PA (EB-PA; OMIM accession no. 226730), who are born with an extremely fragile skin (Charlesworth et al., 2003; Pfendner and Uitto, 2005). As most of these patients harbored premature termination codon or nonsense mutations in exons encoding N-terminal parts of the protein, a rapid decay of the prematurely terminated short RNA transcripts formed is very likely, leading to a complete absence of the protein (Charlesworth et al., 2003). EB-PA mutations being located upstream of exon 31 [the exon encoding plectin's rod domain (Liu et al., 1996)] could therefore not be compensated for by rodless plectin isoforms, explaining the more severe phenotype of patients with plectin-associated EB-PA, compared with patients suffering from EB-MD. Thus, mice with a specific deletion of plectin in stratified epithelia, such as our K5-Cre KO mice, can be considered as an ideal model for the stratified epithelia phenotypes of patients with severe forms of plectin-associated EB-PA.

Before dying, K5-Cre KO mice became progressively weaker, ceased to grow and apparently became unable to suckle, as their stomachs remained empty. Inspection of the oral cavities of newborn K5-Cre KO mice after at least one nursing showed the presence of multiple blisters on their palates and in some cases also on their tongues. Therefore, we reason that the mechanical stress applied to the oral epithelia by sucking and swallowing was the cause of the oral blister formation. As a consequence, the pups' desire for food was probably reduced due to pain and possibly obstruction of the oral cavity by especially large blisters or cellular debris. A similar runting due to prevention of feeding by erosive mucosal blistering was described for mice lacking desmoglein 3 (Koch et al., 1997). In these mice, lesions were initially caused by sucking and became even worse when growing mice began eating solid food. The finding that K5-Cre KO mice did not show epithelial detachment in the esophagus was not surprising, as the liquid diet of neonatal mice exerts only low mechanical stress on such organs.

Mucosal involvement is common in various forms of EB and cases of mucosal blistering associated with EB-MD (OMIM accession no. 226670) have been described (Kunz et al., 2000; Schara et al., 2004). The mouth and throat problems of patients suffering from EB have been reported to often cause a serious disruption of nutrient intake, similar to what we observed with K5-Cre KO mice. Because of oral blistering these children barely grow, as there is a higher need for nutrients because the body loses proteins along with the wound exudate and also has to sustain normal metabolism (information available at the DEBRA website: www.debra-international.org). Pyloric atresia manifests with gastric abnormalities, primarily pyloric and duodenal atresia. However, in K5-Cre KO mice, the movement of coagulated milk from the pylorus into the intestine was not obstructed and consequently, the stomachs were not distended, ruling out that conditional knockout animals were suffering from pyloric atresia. Moreover, the absence of gastric pathologies in K5-Cre KO mice proved the targeting of the plectin gene to be exclusive for stratified epithelia, without affecting simple epithelia.

Even though the epidermis of OHT-treated *Plec*$^{flox/-}$:K5-Cre-ER^{T} mice showed only a mosaic pattern of plectin deletion, its susceptibility towards mechanical stress-induced damage was found to be clearly increased. Evidently, the patchwise deletion of plectin rendered the epidermis more prone to trauma, as

revealed by increased TEWL and lesion formation. The observed more readily removable cells of the deeper epidermal cell layers by tape stripping may also be related to the lesion formation, although reduced cohesion of keratinocytes in the outer epidermal layers due to weakened desmosomal connections cannot be ruled out at the present stage.

Although we used quite high concentrations of OHT to activate Cre recombinase, plectin deletion was achieved only in patches of adult mouse epidermis. Inducible deletion of floxed genes in adult mice via Cre-ER^{T} recombinase is not always 100% effective and appears to be especially difficult to achieve when cytoskeleton-associated proteins with a long half-life are targeted (López-Rovira et al., 2005). The very low turn-over rate of plectin in polarized epithelia (Eger et al., 1997) might explain the relatively weak deletion of plectin expression 14 days after Cre activation, since Cre is activated within 24 hours of the final OHT treatment (Indra et al., 1999). It might be advantageous for future studies to use K14-Cre-ER^{T2} mice, in which induction efficiency is more potent than in K5-Cre-ER^{T} mice (Indra et al., 1999), and to combine this approach with topical application of OHT, which is less toxic than intraperitoneal injection (Vasioukhin et al., 1999) and can be done over longer periods (Benitah et al., 2005). Once more efficient deletion of plectin in adult stratified epithelia has been achieved, it will be interesting to re-evaluate skin barrier function, and moreover, investigate other yet unaddressed skin-related topics, such as wound healing and hair growth.

In summary, the generation of conditional stratified epithelia-specific plectin knockout mice has improved our understanding of the phenotypic manifestations of plectin deficiency in multilayered epithelia. Most importantly, the generation of mice carrying floxed plectin alleles makes it now possible to analyze the function of plectin in various other tissues known to be affected by EB-MD, such as skeletal muscle and brain. In addition, by refining the inducible knockout of plectin in skin, deeper insights into plectin functions in the adult organism might be gained, and a test system for the development of therapeutic approaches for skin-blistering in EB-MD/EB-PA might be obtained.

Materials and Methods

All experiments involving animals were performed in accordance with Austrian Federal Government laws and regulations.

Engineering of plectin conditional knockout mice

To prepare the targeting construct, an FRT-PGKneo^{r}-FRT sequence plus a *loxP* site were inserted into intron 25 of the C-terminal part of the plectin gene. A second *loxP* site was introduced into intron 31. The targeting construct (linearized with *Sal*I) was electroporated into E14.1 embryonic stem cells. Colonies resistant to geneticin (G418) were screened for the desired homologous recombination by Southern blotting. To generate chimeric mice, two recombinant ES cell clones (10-15 cells) harboring the conditional allele of the plectin gene (*Plec*$^{flox(neo)}$) were injected into blastocysts (isolated from C57BL/6 mice at day 3.5 postcoitum; p.c.) that were transferred into pseudopregnant C57BL/6 × CBA females (3.5 day p.c.). A chimeric male offspring was then mated with C57BL/6 mice. Agouti coat-colored offspring was screened for the presence of the *Plec*$^{flox(neo)}$ allele by PCR analysis of tail DNA, using the primers Neo3086 (5′-TCGGCAGGAGCAAGGTGAGATG-3′), pleIn25-26U (5′-GTATTTGGATTCAGAGGCACAGTA-3′) and pleEx26L (5′-CTTCAAGCTCTTGGAGAGTGGCAGG-3′), specific for neo^{r}, intron 25 and exon 26, respectively. Heterozygous mice were bred to FLP deleter mice and offspring was screened for the excised *neo*^{r} gene using primers pleIn25-26U and pleEx26L. After intercrossing mice that were heterozygous for the floxed *Plec* allele (*Plec*$^{+/flox}$), homozygous mice were used to generate animals (*Plec*$^{\Delta/\Delta}$:K5-Cre) that were transgenic for the K5-Cre recombinase and carried the deletion alleles of the plectin gene. The K5-Cre transgene was detected by PCR amplification with the primers Cre sense (5′-CCAATTTACTGACCGTACACC-3′) and Cre antisense (5′-TAATCGCCATCTTCCAGCAGG-3′). The removal of exon 26 to exon 31 by Cre-mediated recombination was confirmed by Southern blotting and PCR analysis using primers pleIn25-26U and pleEx32/L7714 (5′-GCAGCCGCTGGTTTT-CCTCCGCCA-3′).

Preparation of 4-hydroxy-tamoxifen solutions

A 10 mg/ml 4-hydroxy-tamoxifen (OHT; Sigma) solution was prepared as described previously (Metzger and Chambon, 2001). Mice were injected with 1 mg OHT per day for 5 consecutive days.

Antibodies

For a complete list of primary antibodies refer to Table S1 in supplementary material. All secondary antibodies were purchased from Jackson Immuno-Research Laboratories (West Grove, PA).

Immunofluorescence and phase contrast microscopy of tissue sections, apoptosis assay, and dye penetration assay

Tissues were fixed in 4% paraformaldehyde in PBS and embedded in paraffin, or shock frozen in isopentane (cooled with liquid N_2), sectioned (2 μm) on a cryomicrotome, and fixed in acetone at –20°C (Spazierer et al., 2006). Samples were examined using a Zeiss fluorescence laser-scanning microscope (LSM 510) or a Zeiss Axiophot microscope equipped with an AxioCam Hrc camera (Zeiss). Digital images were processed using Adobe Photoshop and Adobe Illustrator software.

Apoptosis was analyzed using the DeadEnd™ Fluorimetric TUNEL System (Promega, Madison, WI). Dye penetration assays were performed as described previously (Spazierer et al., 2006).

Preparation of cell and tissue extracts, and immunoblotting

Epidermis and dermis from newborn mice were separated by treatment with dispase (30 minutes, 37°C), frozen in liquid nitrogen and pulverized. Tissue homogenates were prepared in Triton X-100 high-salt buffer (Eger et al., 1997) by mechanical disruption using a Polytron PT-3000 homogenizer (Kinematica, Littau-Luzern, Switzerland). Cell fractions were obtained from ground frozen tissue following the protocol of Vasioukhin et al. (Vasioukhin et al., 2001). Proteins were subjected to SDS-PAGE and immunoblotting as previously described (Spazierer et al., 2006).

Tape stripping, protein removal assay and TEWL

Tape stripping and measurement of transepidermal water loss (TEWL) were performed as described previously (Spazierer et al., 2006). TEWL of 1-day-old mice was measured with a Tewameter TM-300 equipped with a small-diameter (3 mm) probe, and measurements were digitally recorded via a MPA5 mulitprobe adapter (Courage and Khazaka, Cologne, Germany). The amount of protein removed per D-Squame disk (CuDerm corporation, Dallas, TX) was measured by a modification of the method of Dreher et al. (Dreher et al., 1998). Disks from two subsequent strippings were combined and the NaOH-soluble protein content after neutralization with HCl was determined using the Bio-Rad Protein Assay Kit. Absorption was measured with a spectrophotometer at 595 nm. An empty D-Squame disk and distilled water incubated with the Bio-Rad dye, served as negative controls. The amount of protein measured was then normalized to skin surface area (μg/cm^2).

We thank Manfred Kraus (University of Cologne, Germany) for the neomycin resistance cassette, Junji Takeda (Osaka University, Japan) for providing K5-Cre mouse lines, and Steven Kennel (Oak Ridge National Laboratory, TN) and Takashi Hashimoto (Kurume University School of Medicine, Japan) for antibodies. The help of Fritz Zschiegner (Medical University of Innsbruck, Austria) in anesthetizing mice is greatly appreciated. This work was supported by a grant from DEBRA UK, except for the initial part (generation of *Plec*$^{flox/flox}$ mice) which was supported by grant F 006-11 from the Austrian Science Research Fund.

References

Abrahamsberg, C., Fuchs, P., Osmanagic-Myers, S., Fischer, I., Propst, F., Elbe-Bürger, A. and Wiche, G. (2005). Targeted ablation of plectin isoform 1 uncovers role of cytolinker proteins in leukocyte recruitment. *Proc. Natl. Acad. Sci. USA* **102**, 18449-18454.

Andrä, K., Lassmann, H., Bittner, R., Shorny, S., Fässler, R., Propst, F. and Wiche, G. (1997). Targeted inactivation of plectin reveals essential function in maintaining the integrity of skin, muscle, and heart cytoarchitecture. *Genes Dev.* **11**, 3143-3156.

Andrä, K., Nikolic, B., Stöcher, M., Drenckhahn, D. and Wiche, G. (1998). Not just scaffolding: plectin regulates actin dynamics in cultured cells. *Genes Dev.* **12**, 3442-3451.

Andrä, K., Kornacker, I., Jörgl, A., Zörer, M., Spazierer, D., Fuchs, P., Fischer, I. and Wiche, G. (2003). Plectin-isoform-specific rescue of hemidesmosomal defects in plectin (–/–) keratinocytes. *J. Invest. Dermatol.* **120**, 189-197.

Benitah, S. A., Frye, M., Glogauer, M. and Watt, F. M. (2005). Stem cell depletion through epidermal deletion of Rac1. *Science* **309**, 933-935.

Byrne, C. and Fuchs, E. (1993). Probing keratinocyte and differentiation specificity of the human K5 promoter in vitro and in transgenic mice. *Mol. Cell. Biol.* **13**, 3176-3190.
Charlesworth, A., Gagnoux-Palacios, L., Bonduelle, M., Ortonne, J. P., De Raeve, L. and Meneguzzi, G. (2003). Identification of a lethal form of epidermolysis bullosa simplex associated with a homozygous genetic mutation in plectin. *J. Invest. Dermatol.* **121**, 1344-1348.
Chidgey, M., Brakebusch, C., Gustafsson, E., Cruchley, A., Hail, C., Kirk, S., Merritt, A., North, A., Tselepis, C., Hewitt, J. et al. (2001). Mice lacking desmocollin 1 show epidermal fragility accompanied by barrier defects and abnormal differentiation. *J. Cell Biol.* **155**, 821-832.
Coulombe, P. A., Tong, X., Mazzalupo, S., Wang, Z. and Wong, P. (2004). Great promises yet to be fulfilled: defining keratin intermediate filament function in vivo. *Eur. J. Cell Biol.* **83**, 735-746.
DiPersio, C. M., van der Neut, R., Georges-Labouesse, E., Kreidberg, J. A., Sonnenberg, A. and Hynes, R. O. (2000). Alpha3beta1 and alpha6beta4 integrin receptors for laminin-5 are not essential for epidermal morphogenesis and homeostasis during skin development. *J. Cell Sci.* **113**, 3051-3062.
Dowling, J., Yu, Q. C. and Fuchs, E. (1996). Beta4 integrin is required for hemidesmosome formation, cell adhesion and cell survival. *J. Cell Biol.* **134**, 559-572.
Dreher, F., Arens, A., Hostynek, J. J., Mudumba, S., Ademola, J. and Maibach, H. I. (1998). Colorimetric method for quantifying human stratum corneum removed by adhesive-tape stripping. *Acta Derm. Venereol.* **78**, 186-189.
Eger, A., Stockinger, A., Wiche, G. and Foisner, R. (1997). Polarisation-dependent association of plectin with desmoplakin and the lateral submembrane skeleton in MDCK cells. *J. Cell Sci.* **110**, 1307-1316.
Feil, R., Brocard, J., Mascrez, B., LeMeur, M., Metzger, D. and Chambon, P. (1996). Ligand-activated site-specific recombination in mice. *Proc. Natl. Acad. Sci. USA* **93**, 10887-10890.
Green, K. J. and Gaudry, C. A. (2000). Are desmosomes more than tethers for intermediate filaments? *Nat. Rev. Mol. Cell Biol.* **1**, 208-216.
Guo, L., Degenstein, L., Dowling, J., Yu, Q. C., Wollmann, R., Perman, B. and Fuchs, E. (1995). Gene targeting of BPAG1: abnormalities in mechanical strength and cell migration in stratified epithelia and neurologic degeneration. *Cell* **81**, 233-243.
Indra, A. K., Warot, X., Brocard, J., Bornert, J. M., Xiao, J. H., Chambon, P. and Metzger, D. (1999). Temporally-controlled site-specific mutagenesis in the basal layer of the epidermis: comparison of the recombinase activity of the tamoxifen-inducible Cre-ER(T) and Cre-ER(T2) recombinases. *Nucleic Acids Res.* **27**, 4324-4327.
Koch, P. J., Mahoney, M. G., Ishikawa, H., Pulkkinen, L., Uitto, J., Shultz, L., Murphy, G. F., Whitaker-Menezes, D. and Stanley, J. R. (1997). Targeted disruption of the pemphigus vulgaris antigen (desmoglein 3) gene in mice causes loss of keratinocyte cell adhesion with a phenotype similar to pemphigus vulgaris. *J. Cell Biol.* **137**, 1091-1102.
Kunz, M., Rouan, F., Pulkkinen, L., Hamm, H., Jeschke, R., Bruckner-Tuderman, L., Brocker, E. B., Wiche, G., Uitto, J. and Zillikens, D. (2000). Mutation reports: epidermolysis bullosa simplex associated with severe mucous membrane involvement and novel mutations in the plectin gene. *J. Invest. Dermatol.* **114**, 376-380.
Liu, C. G., Maercker, C., Castanon, M. J., Hauptmann, R. and Wiche, G. (1996). Human plectin: organization of the gene, sequence analysis, and chromosome localization (8q24). *Proc. Natl. Acad. Sci. USA* **93**, 4278-4283.
López-Rovira, T., Silva-Vargas, V. and Watt, F. M. (2005). Different consequences of beta1 integrin deletion in neonatal and adult mouse epidermis reveal a context-dependent role of integrins in regulating proliferation, differentiation, and intercellular communication. *J. Invest. Dermatol.* **125**, 1215-1227.
Mahrle, G., Schulze, H. J., Kuhn, A. and Wevers, A. (1989). Immunostaining of keratin and vimentin in epidermis: comparison of different post-embedding immunogold techniques for electron microscopy. *J. Histochem. Cytochem.* **37**, 863-868.
Metzger, D. and Chambon, P. (2001). Site- and time-specific gene targeting in the mouse. *Methods* **24**, 71-80.
Peters, B., Kirfel, J., Bussow, H., Vidal, M. and Magin, T. M. (2001). Complete cytolysis and neonatal lethality in keratin 5 knockout mice reveal its fundamental role in skin integrity and in epidermolysis bullosa simplex. *Mol. Biol. Cell* **12**, 1775-1789.
Pfendner, E. and Uitto, J. (2005). Plectin gene mutations can cause epidermolysis bullosa with pyloric atresia. *J. Invest. Dermatol.* **124**, 111-115.
Pfendner, E., Rouan, F. and Uitto, J. (2005). Progress in epidermolysis bullosa: the phenotypic spectrum of plectin mutations. *Exp. Dermatol.* **214**, 241-249.
Raymond, K., Kreft, M., Janssen, H., Calafat, J. and Sonnenberg, A. (2005). Keratinocytes display normal proliferation, survival and differentiation in conditional beta4-integrin knockout mice. *J. Cell Sci.* **118**, 1045-1060.
Rezniczek, G. A., de Pereda, J. M., Reipert, S. and Wiche, G. (1998). Linking integrin alpha6beta4-based cell adhesion to the intermediate filament cytoskeleton: direct interaction between the beta4 subunit and plectin at multiple molecular sites. *J. Cell Biol*. **141**, 209-225.
Schara, U., Tucke, J., Mortier, W., Nüsslein, T., Rouan, F., Pfendner, E., Zillikens, D., Bruckner-Tuderman, L., Uitto, J., Wiche, G. et al. (2004). Severe mucous membrane involvement in epidermolysis bullosa simplex with muscular dystrophy due to a novel plectin gene mutation. *Eur. J. Pediatr.* **163**, 218-222.
Schoch, K. G., Lori, A., Burns, K. A., Eldred, T., Olsen, J. C. and Randell, S. H. (2004). A subset of mouse tracheal epithelial basal cells generates large colonies in vitro. *Am. J. Physiol. Lung Cell. Mol. Physiol.* **286**, 631-642.
Spazierer, D., Fuchs, P., Reipert, S., Fischer, I., Schmuth, M., Lassmann, H. and Wiche, G. (2006). Epiplakin is dispensable for skin barrier function and for integrity of keratin network cytoarchitecture in simple and stratified epithelia. *Mol. Cell. Biol.* **26**, 559-568.
Swensson, O., Langbein, L., McMillan, J. R., Stevens, H. P., Leigh, I. M., McLean, W. H., Lane, E. B. and Eady, R. A. (1998). Specialized keratin expression pattern in human ridged skin as an adaptation to high physical stress. *Br. J. Dermatol.* **139**, 767-775.
Tarutani, M., Itami, S., Okabe, M., Ikawa, M., Tezuka, T., Yoshikawa, K., Kinoshita, T. and Takeda, J. (1997). Tissue-specific knockout of the mouse Pig-a gene reveals important roles for GPI-anchored proteins in skin development. *Proc. Natl. Acad. Sci. USA* **94**, 7400-7405.
Vasioukhin, V., Degenstein, L., Wise, B. and Fuchs, E. (1999). The magical touch: genome targeting in epidermal stem cells induced by tamoxifen application to mouse skin. *Proc. Natl. Acad. Sci. USA* **96**, 8551-8556.
Vasioukhin, V., Bowers, E., Bauer, C., Degenstein, L. and Fuchs, E. (2001). Desmoplakin is essential in epidermal sheet formation. *Nat. Cell Biol.* **3**, 1076-1085.
Wiche, G. (1998). Role of plectin in cytoskeleton organization and dynamics. *J. Cell Sci.* **111**, 2477-2486.

Journal of Cell Science

Table S1. Primary antibodies used for immunoblotting

Antigen	Antibody	Vendor/Catalog# Reference/Name or Clone#	Dilution
Actin	mouse mAb	Sigma-Aldrich, Austria/clone AC-40	1:500
Desmoplakin	mouse mAb	Progen, Heidelberg, Germany/clones DP-2.15, DP-2.17, DP-2.20	1:400
E-Cadherin	mouse mAb	BD Transduction Laboratories, Lexington, KY/clone 36	1:2000
Fodrin	mouse mAb	Signet Laboratories, Dedham, MA/clone D8B7	1: 500
Involucrin	rabbit antiserum,	Covance, Princeton, NJ/PRB-140C	1:1000
Integrin β4	rabbit antiserum	Santa Cruz Biotechnology, Santa Cruz, CA/H-101	1:200
Keratin 5	rabbit antiserum	Covance, Princeton, NJ/PR-B160-P	1:1000
Keratin 6	rabbit antiserum	Covance, Princeton, NJ/PR-B169-P	1:2000
Plectin (N-terminal domain)	rabbit antiserum	Andrä et al., 2003/antiserum #9	1:3000
Tubulin (alpha)	mouse mAb	Sigma-Aldrich, Austria/clone 5-B-12	1:2000

Primary antibodies used for immunofluorescence microscopy

Antigen	Antibody	Vendor/Catalog# Reference/Name or Clone#	Dilution
BPAG1	mouse mAb	Hashimoto et al., 1993/clone Mab-5E	1:100
Desmoplakin	mouse mAb	Progen, Heidelberg, Germany/clones DP-2.15, DP-2.17, DP-2.20	undiluted
E-Cadherin	mouse mAb	BD Transduction Laboratories, Lexington, KY/clone 36	1:100
Integrin β4	rat mAb	Kennel et al., 1989/clone 346-11A	1:100
Involucrin	rabbit antiserum	Covance, Princeton, NJ/PRB-140C	1:1000
Keratin 5	rabbit antiserum	Covance, Princeton, NJ/PR-B160-P	1:800
Keratin 6	rabbit antiserum	Covance, Princeton, NJ/PR-B169-P	1:500
Keratin 10	mouse mAb	Chemicon, Temecula, CA/clone MAB3230	1:400
Keratins 5,6,18	mouse mAb	Dako-Cytomation, Glostrup, Denmark/clone LP34	1:100
Ki-67	mouse mAb	Dako-Cytomation, Glostrup, Denmark/clone TEC-3	1:50
Plectin (rod domain)	rabbit antiserum	Andrä et al., 2003/antiserum #46	1:100